Effects of Electromagnetic and Hydraulic Forming Processes on the Microstructure of the Material *

Fr. W. Bach[1], L. Walden[1], M. Kleiner[2], D. Risch[2]

[1] Institute of Materials Science, University of Hannover, Germany
[2] Chair of Forming Technology, University of Dortmund, Germany

Abstract

Over the past few years, various papers have been published in the field of high speed forming processes. The focus was mainly on the technological aspects of metal forming, however. Therefore, the present contribution puts an emphasis on transmission electron microscopy analyses.

The present research work describes the effects of the two forming processes upon the aluminum microstructure and their influence on the material properties. The objective is to characterise the micro processes determining the plastic deformation with both forming velocities – the electromagnetic high speed forming process with strain rates of 10,000 s^{-1} and the bulge test, having deformation rates of less than 0.1 s^{-1} as a quasi-static process. In this article sheet metals out of technical pure aluminum 99.5% with a thickness of 1 mm were investigated. To this end, sample specimens were taken from manufactured workpieces along the radius at various distances from the center. Because of the similarity of the forming paths, two places on the specimens manufactured at different forming rates were evaluated and compared to each other: immediately next to the blankholder and from the area of maximum strain. Metallographic tests of the structures, the sheet thickness, and the micro hardness distribution of the initial state and the formed sheet metals were executed in advance.

Keywords:

Electromagnetic sheet metal forming, Bulge test, Microstructure, Dislocation

---

* *This work is based on the results of FOR443; the authors would like to thank DFG for its financial support*

1 Introduction

Electromagnetic sheet metal forming (EMF) is a typical high speed forming process using the energy density of a pulsed magnetic field for a contactless forming of metals with high electrical conductivity, such as aluminum or copper. During this process maximum strain rates of 10,000 s^{-1} are achievable. As known from the literature, the material behavior at these high strain rates differs significantly from the one at quasi-static loading with deformation rates lesser than 0.1 s^{-1} [1]. Phenomenological observations during experiments indicate that the material seems to have a higher strength and greater formability under high speed forming conditions [2]. To evaluate the influence of the forming velocity, an investigation of two processes with different maximum strain rates was performed, especially to analyse the resulting material microstructure. The first process was the electromagnetic sheet metal forming as mentioned before. Secondly, the bulge test, using a pressurised fluid medium in order to obtain the deformation, was considered as a quasi-static process. The process principles and parameters are shown in Figure 1.

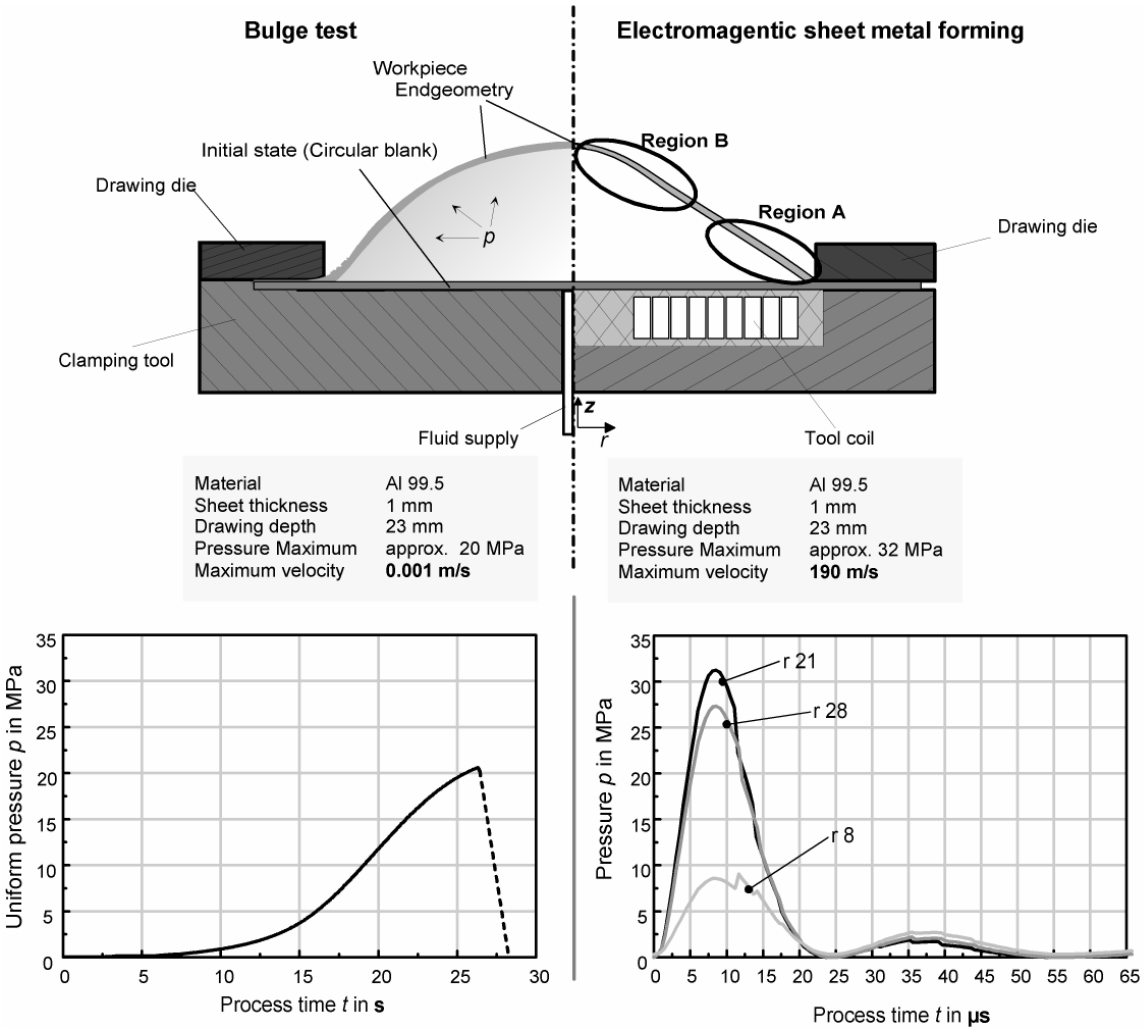

Figure 1: *Process principles and relevant parameters*

The pressure impulse in the electromagnetic sheet metal forming is very high and exists only in a short time slot. In contrast to this, the pressure impulse in the bulge test is long compared to the process time and has a smaller maximum. Furthermore, the pressure impulse in the EMF is a function over time and radius (see Figure 1), contrary to the pressure impulse in the bulge test which depends only on time. But both processes produce a similar final geometry. Only the deformation process differs significantly with respect to the occurring strain paths. Distinctive bending and unbending processes were present in area B during the EMF-process, whereas a constant stretch-forming condition exists during the bulge test. Comparable strain paths are observable only in region A for both processes. Despite of this, the whole developed lengths of the specimens was analysed in order to obtain information about the microstructure, because maximum strain rates occur in area A during the EMF-process.

If an external force is applied upon the workpiece the deformation of the material is caused by a slipping of atom layers in defined crystallographic directions and planes corresponding to the shear stress. Interaction between crystal defects, such as dislocations and the surrounding crystal lattice, are decisive for plastic deformation. Dislocations are linear lattice defects developing in slip planes and moving through the lattice driven by the outside force. According to the crystal plasticity theory, deformation takes place due to the migration of dislocations. This, in turn, increases the dislocation density depending on various mechanisms producing further dislocations. An increase of the yield stress because of intensified hardening at rising strain rates as well as a higher breaking elongation of the material are characteristic for the high speed forming process. On the microstructural level, aside from the thermally activatable deformation mechanisms, damping mechanisms occur at deformation rates of 10,000 s^{-1}. Slip obstacles are overcome non-thermally, without dwell time, too. Therefore, the decisive factor for the deformation based on these mechanisms is not the time needed for overcoming the obstacles, but the run time in between. The resulting greater plastic deformation of the material increases the possibility of the transformation of the microstructure due to the interaction of the dislocations with the grain boundaries, the precipitations, and other dislocations. The dislocation arrangement becomes inhomogeneous, cell structures are formed that change into subgrain boundaries. Only very few experimental studies of dislocation structures at very high strain rates using transmission electron microscopy (TEM) are available, therefore they are represented in detail here. For a complete characterisation of the material, the grain size, the stretching of the grain, the sheet thickness distribution as well as the micro hardness distribution in the initial state and along the radius of the formed specimens were determined. Corresponding specimens were analysed subsequently using the transmission electron microscope and were evaluated regarding their microstructure. In this work, a sheet metal of technically pure aluminum 99.5% with a thickness of 1 mm was analysed. The resultant different microstructure caused by the two considered processes will be analysed and discussed in the following chapters.

2 Metallographic and mechanical investigations

2.1 Microstructural investigations

In order to accomplish a complete analysis of the workpiece, the different laboratory analyses were conducted on different radiuses of the metal sheets in the shaped state. The labels of the inspected areas along the radius can be taken from Figure 2. The labels on the depicted specimen apply to both strain processes. They are adhered to for all subsequent analyses. The names “outer surface” and “inner surface” refer to the tool coil. The surface of the workpiece that faces the tool coil is called the inner surface, the outer surface is the opposite face.

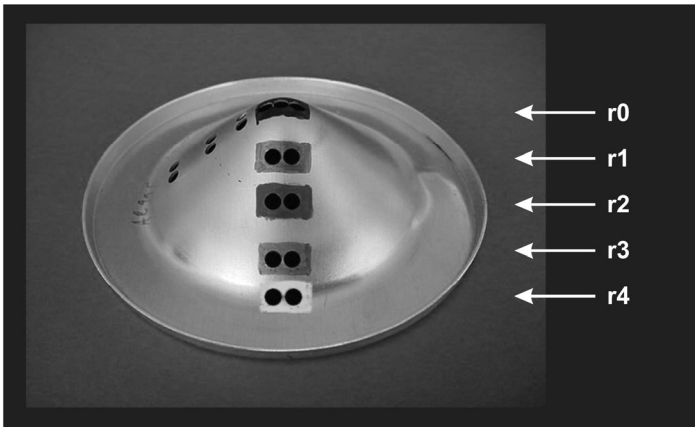

Figure 2: *Electromagnetically formed workpiece; region of interest*

Figure 3 summarises micrographs of the initial state and of the electro-magnetically shaped workpiece. Each depicts a transversal-section of the metal sheet, no particular differences between the surfaces, and the center of the specimen were apparent. Bach et. al describes already summarised analyses of the initial state as well as shaped specimens while varying the process parameters along the rolling direction (RD: rolling direction) [3]. Thus, this paper shows analyses along the transverse direction (TD: transverse direction) for comparison purposes. In the initial state the grains are less stretched in this direction, thus differences in the grain elongation become more obvious. For testing purposes, the electro-magnetically shaped workpiece was divided into two sub-divisions - in the immediate vicinity of the blankholder and from the center of the specimen. The metallographic analyses show a difference in the grain elongation between these areas (quantitatively, cf. chapter 2.2). The grain size remains constant, whereas the grain elongation continuously increases along the radius of the specimen towards the center of the specimen.

The micrographs of the hydraulically shaped specimen are shown in Figure 4. Just like the electro-magnetically shaped workpieces, no changes in the grain size are visible, but a grain elongation does occur. In the flange area (r4) a lower grain elongation than in the areas r3 to r0 occurs (quantitatively, cf. chapter 2.2). The grain elongation in the areas r3 to r0 remains constant as opposed to the electro-magnetically shaped workpiece.

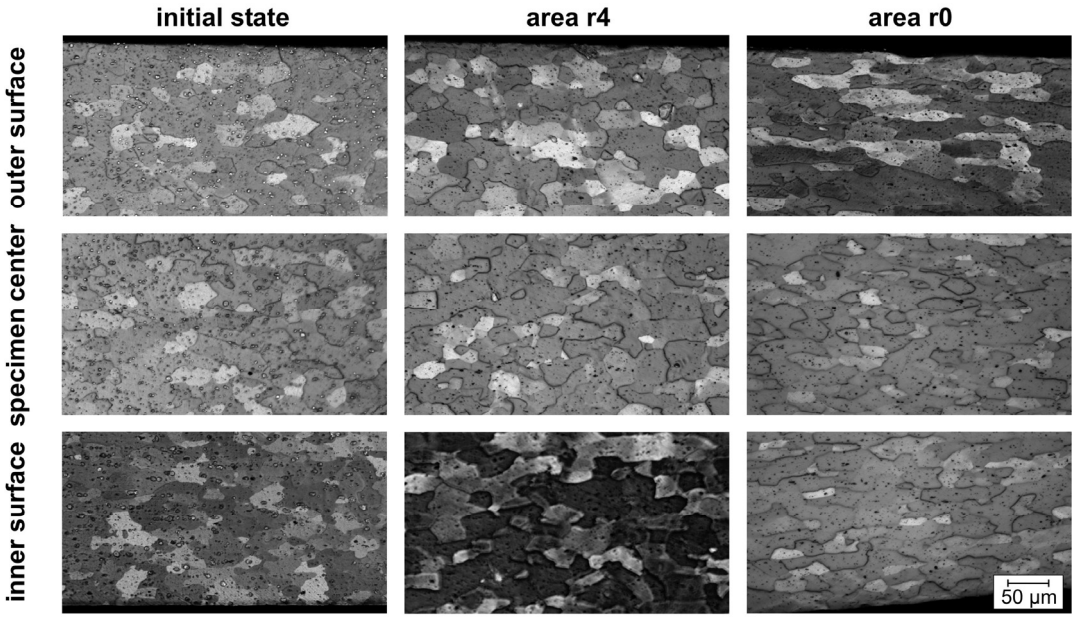

Figure 3: *Microstructure of the initial state and the electromagnetically formed workpiece in TD*

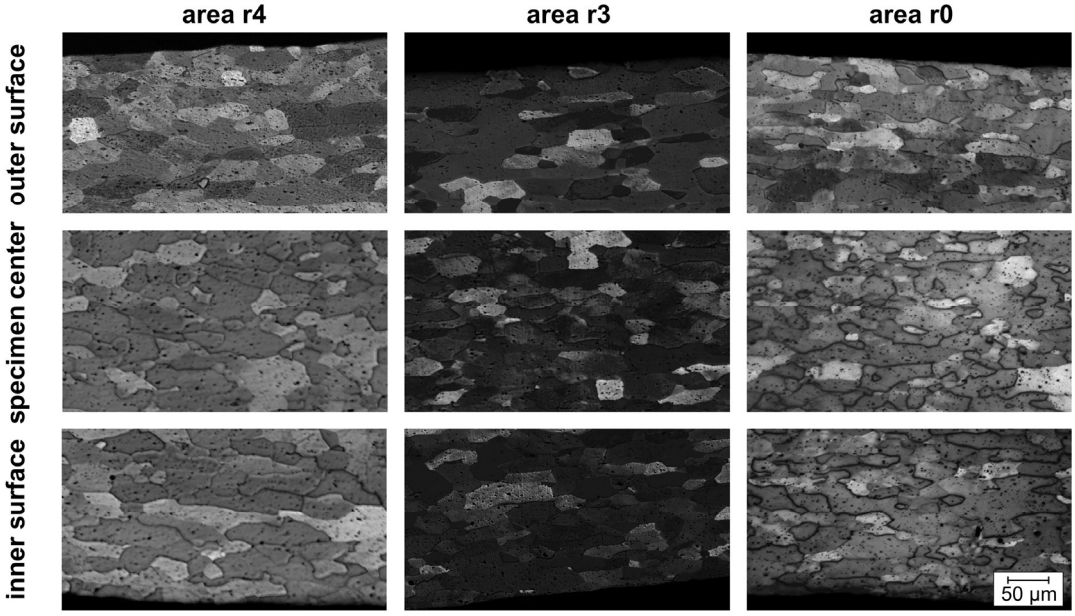

Figure 4: *Microstructure of the hydraulically formed workpiece in TD*

The accomplished metallographic investigations show that both processes cause relatively similar effects on the microstructure, which are expressed in an elongation of the grains along the specimen radius. The difference lies in the extent of the elongation. The aspect ratio of the hydraulically deformed specimen remains constant along the radius. This fact indicates a homogeneous strain. The electromagnetically deformed specimen shows an increased elongation along the radius, which means that in this case the strain varies.

2.2 Grain size and grain stretching

The quantitative evaluation of the ASTM G (G: grain size) by the use of metallographic micrographs is conducted in accordance with the standards ASTM E112 and DIN 50601, using an image processing software. For the analysis, the planimetric process was used. This calculating algorithm is based on a reconstruction of the grain boundaries and is insensitive where bothersome artifacts, such as inclusions and etch effects, are concerned.

Figure 5 shows the results of the grain size and grain elongation evaluation. The grain size is relatively homogenous, its mean value in the initial state is G = 8.4 and for the shaped specimens G = 8.5 ± 0.1. The grain elongation is then calculated as quotient of the vertical and horizontal grain size and is non-dimensional just like the grain size. The elongation of the grains in the initial state is 1.01. For the electro-magnetically shaped workpiece it increases continuously from 0.94 in the flange area (r4) up to 0.85 in the center of the specimen (r0). For the hydraulically shaped specimen the value 0.92 applies for the flange area (r4) and 0.89 in the areas r3 to r0.

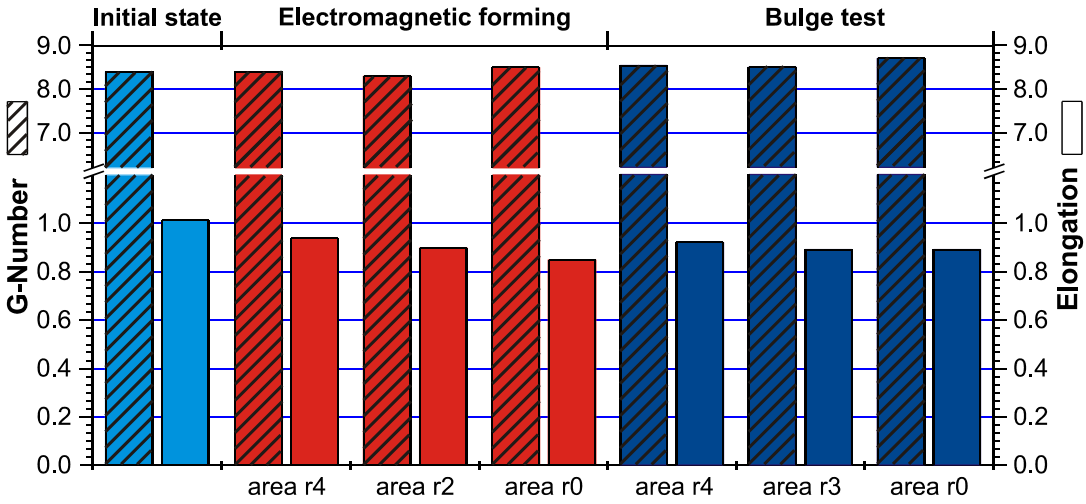

Figure 5: *Grain size and grain stretching of the initial state and both formed workpieces*

The evolution of grain morphology of electro-magnetically and hydraulically shaped specimens has been studied quantitatively. The investigations of the microstructure confirm the results of the analysis of the micrographs concerning the material behaviour.

2.3 Sheet metal thickness distribution

The wall thickness was measured along the radius of the specimens using a stereomicroscope and an image analysis program. For the tested workpieces no obvious difference in the comparison of the specimens taken in and transverse to the rolling direction could be determined (Figure 6). But for both shaping processes a reduction of the wall thickness along the radius in the direction towards the center of the specimen was found. For the hydraulically shaped specimen, the wall thickness decreases more continuously than for the electro-magnetically shaped one. The values of the wall thicknesses in the center of the specimen are identical at 660 ± 10 µm.

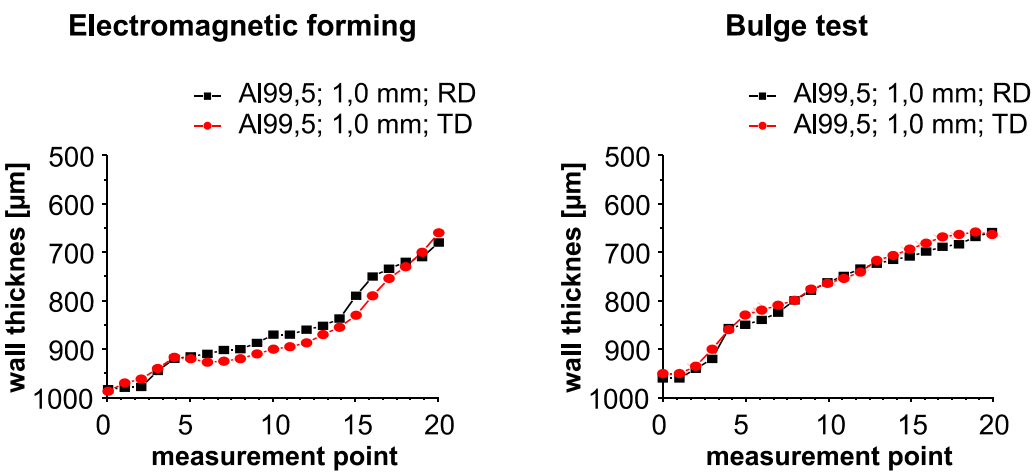

Figure 6: *Sheet metal thickness of the electromagnetically and hydraulically formed workpieces*

2.4 Micro hardness distribution

In the initial state the progression of the hardening depth along the thickness of the metal sheets was measured in order to detect existing differences between edge and center, and to compare these to the values of the shaped specimens (Figure 7, Figure 8 right). The hardness values determined in transversal direction did not show any obvious differences between the outer and the inner surface and the center of the specimen. The mean micro hardness is 29 ± 2 HV 0.5/10.

The electro-magnetically shaped workpiece shows a significant tendency for increased micro-hardness towards the direction of the center of the specimen. The results are shown in Figure 7. In the flange area (r4) it is 54 +/- 4 HV 0.5/10 and in the area r0 71 +/- 2 HV 0.5/10. The values along the thickness of the metal sheets differ and they are higher for the center of the sheet metal than for the outer and inner surface (Figure 7 top).

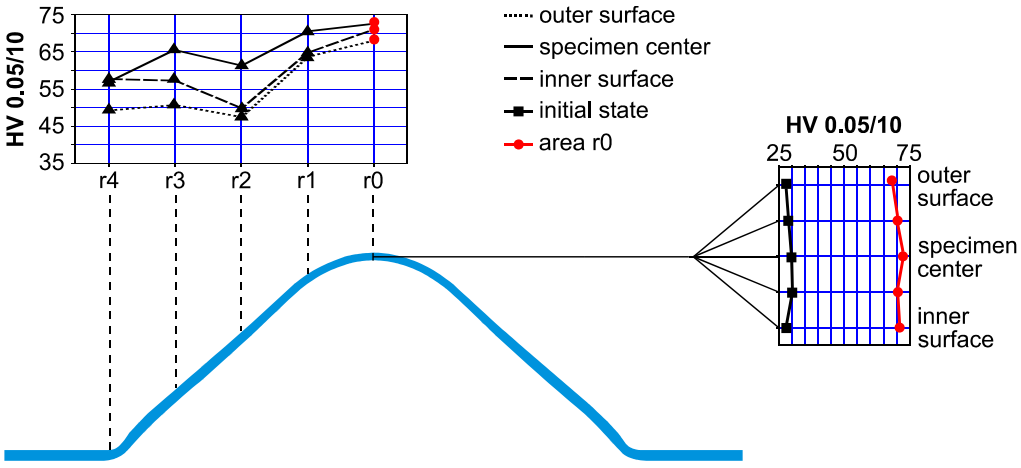

Figure 7: *Micro hardness of the initial state and the electromagnetically formed workpieces in TD*

The progression of the micro-hardening depth of the hydraulically shaped specimen is depicted in Figure 8. Here, an increase in hardness can be observed in comparison to the initial state. This does turn out to be lower than for the electro-magnetically shaped workpiece. The values in the examined areas r4 to r0 are relatively similar and their mean value is in the flange area (r4) 43 HV 0.5/10 and in the area r0 48 HV 0.5/10, there is minor increase in the direction towards the center of the specimen. No differences between the outer and the inner surface become evident in relation to the thickness of the metal sheets.

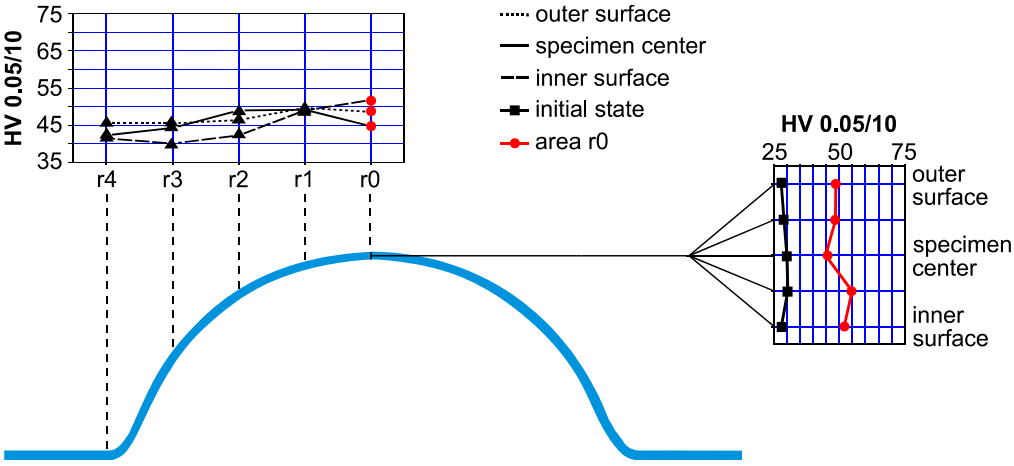

Figure 8: *Micro hardness of the initial state and the hydraulically formed workpieces in TD*

The results of the microhardness investigations indicate (assuming a similar wall thickness of the specimens) that the microhardness values rise as a function of the grain elongation and the strain.

3 TEM investigations

In order to gather a general understanding of the strain mechanisms and to enable a micro-structural modeling of the two strain processes, analyses under the transmission electron microscope (TEM) are necessary. For the individual sampling locations, which are shown in Figure 2, general micrographs with 20.000 and 40.000-fold magnification, respectively, were made. For especially interesting areas detailed micrographs with a magnification of 80.000 to 200.000 were made. Aluminum has a face-centered cubic lattice with 12 slip systems at room temperature. In the poly-crystalline material there are sufficient degrees of freedom to enable an arbitrary plastic deformation.

Figure 9 shows two areas that represent the initial state of the material. In the left part of the figure grain boundaries of a total of five grains can be seen. The TEM cannot produce images of the whole grain, due to the grain size. Because of the different orientations of the crystals, during the preparation of the specimen preparation artifacts occur, and as a result geometrically arranged patterns of the microstructure appear. In the picture, a number of precipitations as well as a few dislocations are visible. In the right part of the Figure 9, next to some dislocations, a sub grain boundary as dislocation orientation is visible. All in all, the dislocation density is very low, which can be explained by a heat treatment in the course of the sheet manufacture.

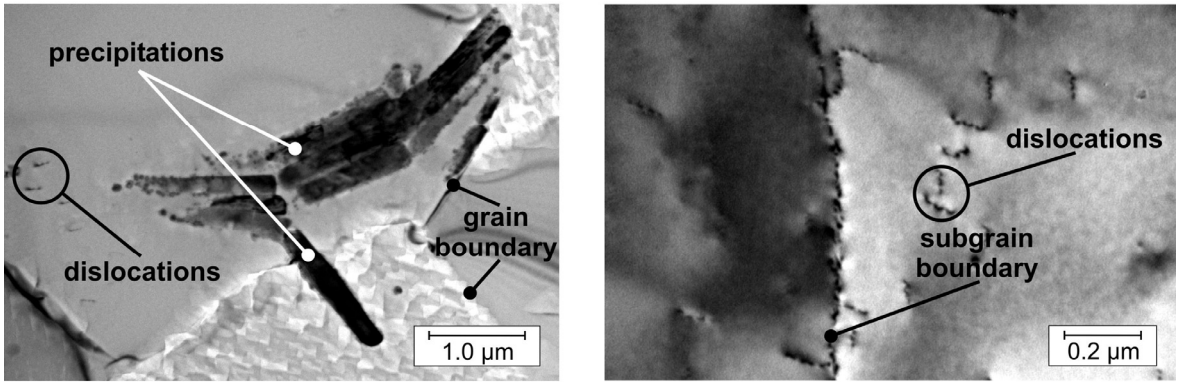

Figure 9: *Microstructure of the initial state*

Figure 10 shows the microstructure pictures of the electro-magnetically shaped work-piece. The specimens were taken from the flange area (r3). The microstructure can be characterised by two representative areas. For one: areas that show a number of single dislocations in comparison with the initial state. But the dislocation density overall is still not very high (Figure 10 top). For two: in parts, dislocation tangles and arrangements of a number of dislocations are visible. These arrangements, however, do not constitute sub-grain boundaries, but coupled dislocation groups.

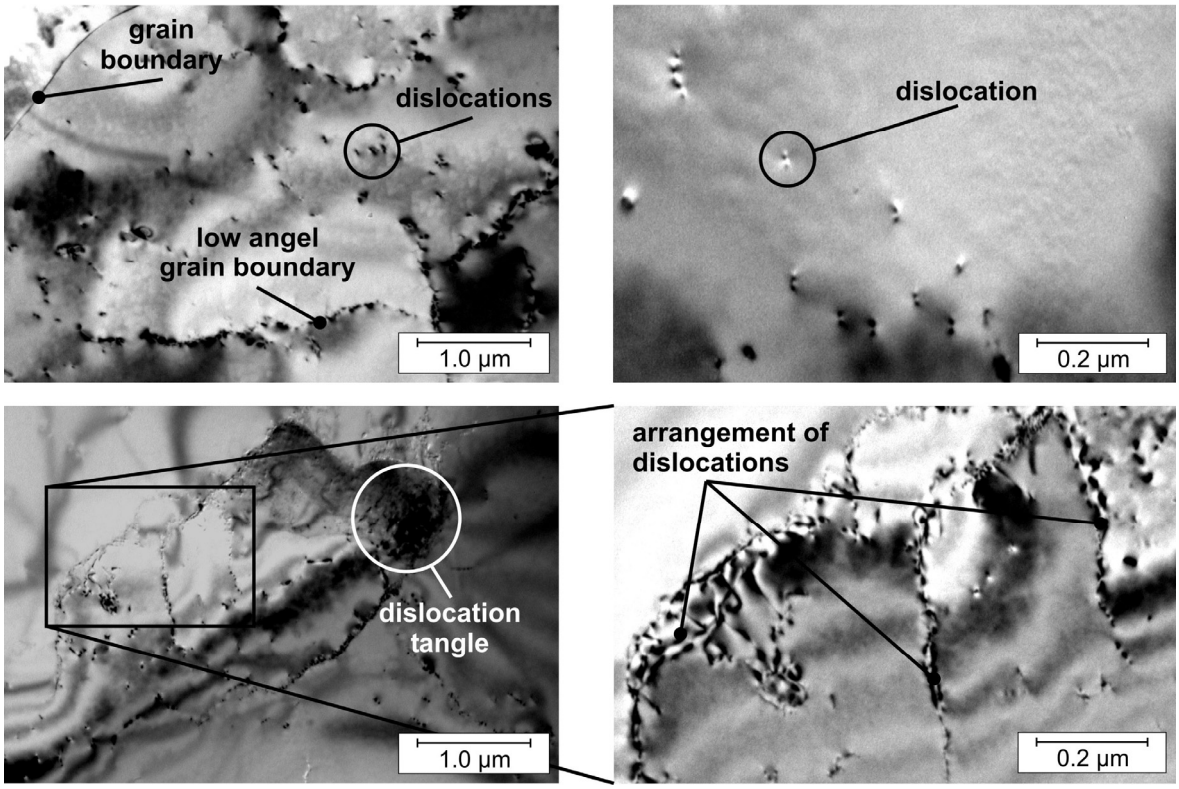

Figure 10: *Microstructure of the electromagnetically formed workpiece near to the flange region (area r3)*

The pictures from the center of the specimen (area r0) of the electro-magnetically shaped specimen are shown in Figure 11. Here, a distinctive cell structure is visible, which is characterised by a low cell wall thickness (Figure 11 top). The differences in contrast that can be seen in Figure 11, top left, indicate orientation differences between the differently defined areas. This means these are subgrains or areas separated by low angle grain boundaries. A number of the areas on the specimen show loosely coupled dislocation groups (Figure 11 bottom left). In many cases dislocation networks are visible (Figure 11 bottom), the cell walls, however, do show in part already subgrain boundary characteristics.

The corresponding areas were also examined on the hydraulically shaped workpiece. Significant differences appeared for the first specimen, which was taken in the vicinity of the blankholder (area r3), are shown in Figure 12. The specimen is characterised by areas with a very high dislocation density (Figure 12 top). A representative picture that shows all dislocations present in a certain area is impossible due to the different orientations of the dislocations. This is also the reason why there are areas in the pictures that seem free of dislocations. For a different tilt angle those areas also show a high dislocation density. There are a number of places with dislocation tangles (Figure 12 bottom left). Rarely, there are areas with a low dislocation density, such as in Figure 12 bottom right.

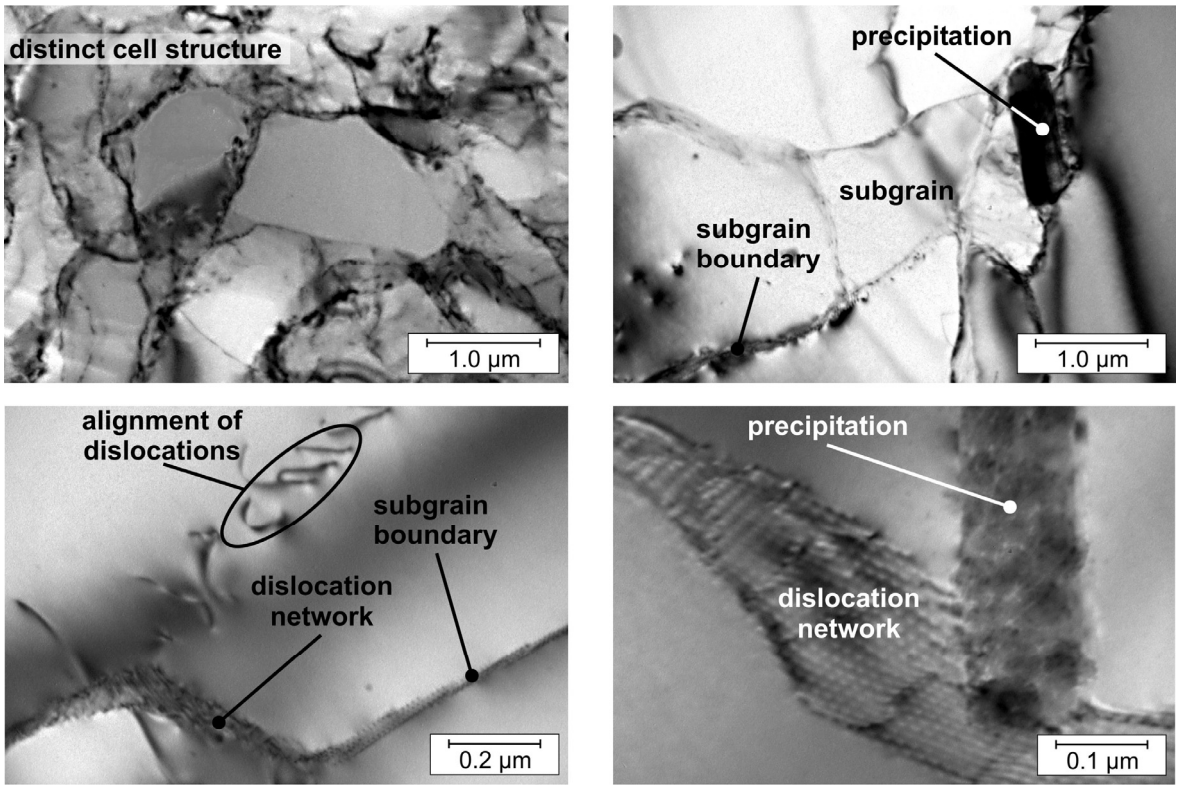

Figure 11: *Microstructure of the electromagnetically formed workpiece - r0 area*

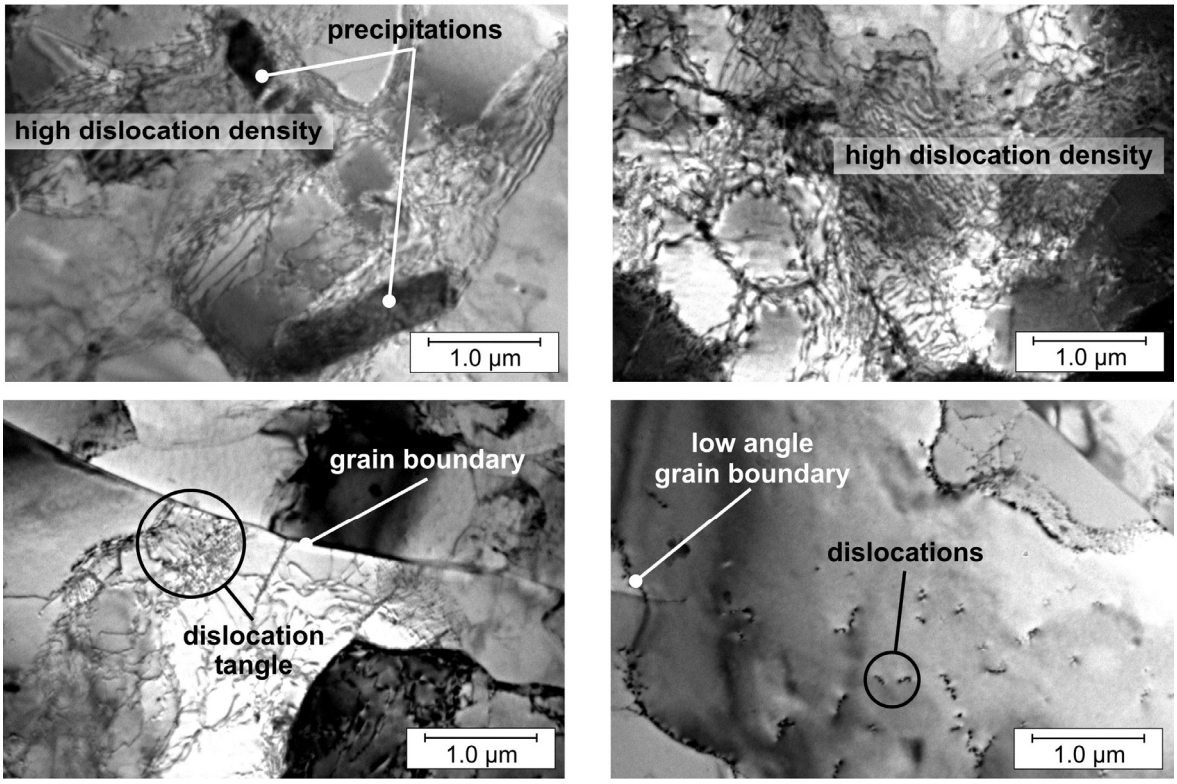

Figure 12: *Microstructure of the hydraulically formed workpiece near to the Blankholder (r3 area)*

The center of the specimen (area r0) of the hydraulically shaped workpiece is depicted in Figure 13. There are significant differences in the comparison of the specimens taken from the flange area. Similarly to the specimens shaped electro-magnetically, the dislocations in these cases establish cell structures. The cells do have thicker walls, though (Figure 13 top right); the interior of the cells again is relatively void of dislocations. These new structures created by the strain in part do not show a difference in contrast, and thus they have only few orientation differences. The two lower pictures show a grain photographed at different tilt angles. In the lower left picture the grain is apparently homogenous; in the right picture it becomes obvious that it is criss-crossed by low angle grain boundaries.

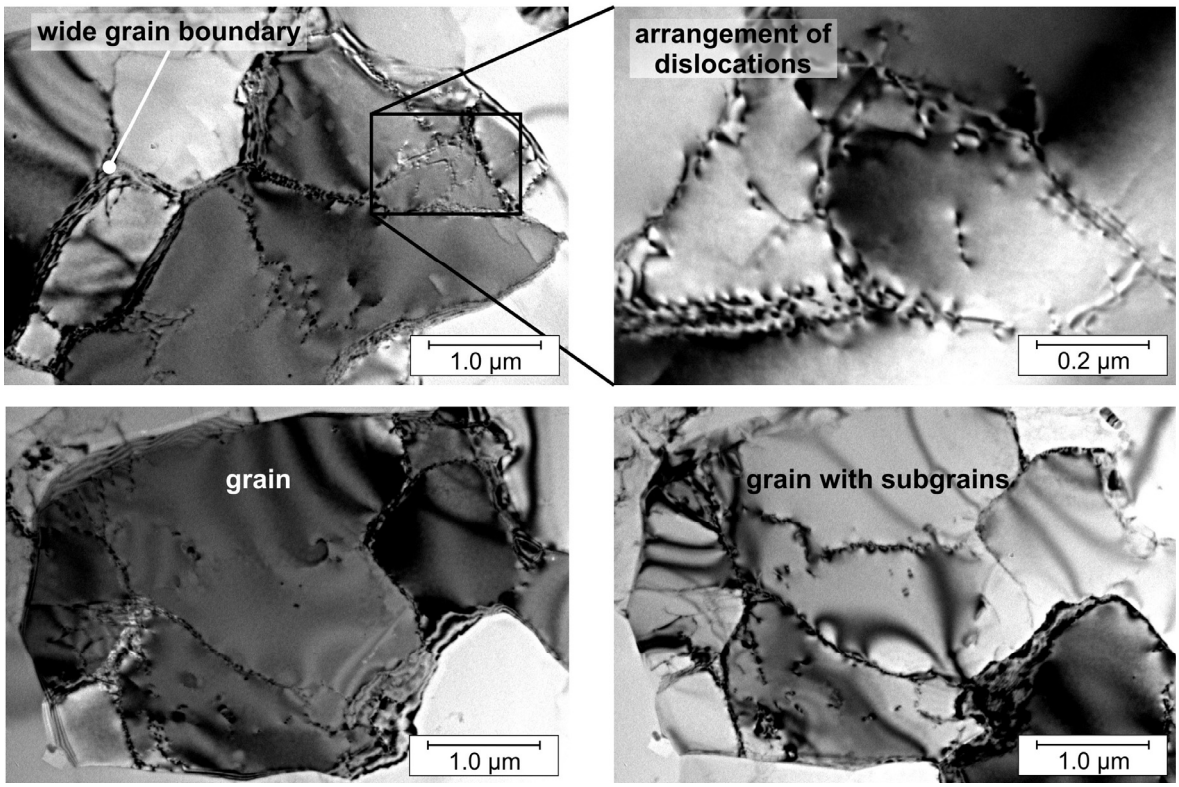

Figure 13: *Microstructure of the hydraulically formed workpiece in the middle of the specimen (r0 area)*

According to the crystal plasticity theory, macroscopic plastic deformation is mainly caused by the creation and the movement of dislocations. In the course of a plastic deformation the dislocation populations undergo several stages of development depending on the degree of straining. According to Honeycombe, these are divided into five areas depending on the strain [4]:

- area I – here mainly primary slip planes become active. Dislocations creep long distances, there is a low dislocation density.
- area II – here also secondary slip planes, active sources, and Lomer-Cottrell-dislocations are activated. There is a high dislocation density. In case of further strain, the dislocations localise and form dislocation tangles, which turn into cell structures.
- area III – here, in addition to the other activating processes, cross-slipping also starts. The three-dimensional structure of the cells turns into a two-dimensional dislocation net. This is the formation mechanism of a subgrain. If the deformation continues the subgrains are elongated and called micro-bands. In case of further deformation, so-called shear bands appear.
- For extreme strains, the areas IV and V can be observed, which are characterised by very distinct recovery mechanisms and a reduction of the established structures.

The transmission electron microscopy analyses of the examined strain processes show typical attributes of a deformation at low temperatures, this means temperatures lower as 0.4 T_s (T_s: melting point). Furthermore, divergent elongations were observed for the two processes. According to the classification by Honeycombe, the electro-magnetically shaped specimen has to be assigned the areas I to III depending on the stress, whereas the hydraulically shaped specimen belongs exclusively to area II.

4 Summary

The aim of the presented analyses is a comparison between two strain processes – the electro-magnetic and the hydraulic straining. The main difference between these processes lies in the type of material treatment. The electro-magnetic straining is a dynamic straining having strain rates of up to 10,000 s^{-1}, whereas the hydraulic straining constitutes a quasi steady-state straining process with strain rates lesser than 0.1 s^{-1}. The examined material was a sheet metal of technically pure 99.5 Aluminum with a thickness of 1 mm. The examined workpieces were strained to the identical draw depth of 23 mm. The analyses were conducted on different areas of the specimen, in order to accomplish a comprehensive characterisation of the strain processes. Next, the results are summarised.

The qualitative and quantitative metallographic analyses show a microstructure with constant grain size. The differences for the shaped specimens become evident mainly in the elongation of the grains. For the electro-magnetically shaped specimen the grain elongation along the radius of the workpiece increases, whereas it remains constant for the hydraulic straining.

The progression of the wall thickness along the radius of the specimen shows a constant decrease towards the center of the workpiece. In case of the hydraulic straining it runs more continuously than for the electro-magnetical one. The center of the specimen shows the least thickness of the metal sheets, it is identical for both types of straining.

The micro hardness increases significantly for the shaped specimens. For the hydraulic strain, the increase in micro hardness is distributed relative continuously over the whole radius of the specimen. In case of the electro-magnetically shaped workpiece, the micro hardness increases along the radius of the specimen towards the center of the specimen. Overall, the micro hardness values for the electro-magnetically shaped workpiece exceed those of the hydraulically shaped ones.

The TEM-analyses show a divergent behavior of the two straining types. Previous publications have shown that the straining of a workpiece occurs according to the crystal plasticity theory through the creation and movement of dislocations. In the course of a strain, at first the dislocation density increases, then the dislocations localise and make up dislocation tangles. Finally, a cell structure is established [5]. In the course of further deformation of the material, the cell size decreases and the interior of the cell becomes increasingly devoid of dislocations. For the hydraulically shaped specimen, interactions of this kind occur. In the flange area the dislocation density is high, towards the center of the specimen a transition into a cell structure occurs. In case the strain increases still, the cell wall thickness is reduced, owing to energetic reasons, and is converted from a three-dimensional to a two-dimensional structure. A dislocation network develops, which constitutes the grain boundary of a subgrain. The dislocation recovery in the interior of the subgrain occurs through the annihilation of dislocation pairs or by absorption at the subgrain

or grain boundaries. The resulting microstructure can be observed in the center of the specimen of the electro-magnetically shaped workpiece. The flange area, on the other hand, shows a comparatively low dislocation density which indicates a low strain. The different strain processes of the workpiece at the edge and in the center also explain the differences in grain elongation and micro hardness. Finally, it can be stated that the microstructural differences between both strain processes result only from the strain rate and the degree of strain. The TEM-analyses clearly show that both these processes are cold-working processes and, furthermore, that the electro-magnetically shaped workpieces signify different strain rates over the radius of the specimen.

References

[1] *Lange, K.* (Hrsg.): Umformtechnik, Vol. 1, Springer-Verlag, Berlin/Heidelberg, 1993.

[2] *Beerwald, C.; Brosius, A.; Homberg, W.; Kleiner, M.; Wellendorf, A.:* New Aspects of Electromagnetic Forming. Proceedings of the 6th International Conference on technology of Placticity, 19.-24. Sept. 1999, Nürnberg, vol. 3, p. 2471-2476.

[3] *Bach, Fr.-W.; Rodman, M.; Rossberg, A.; Weber, J.; Walden, L.:* Verhalten von Aluminiumwerkstoffen bei der elektromagnetischen Blechumformung; 2. Kolloquium elektromagnetische Umformung, 28. Mai 2003 Dortmund, 2003.

[4] *Honeycombe, R.:* The plastic deformation of metals, Edward Arnold Ltd. London, 2. ed., 1984.

[5] *Lan, Y.:* Verfestigungsverhalten und Versetzungsstruktur von Eisen und Aluminium bei niedriger Temperatur. Fortschritts-Berichte VDI, vol. 5, Nr. 249, 1992.